1.56 Terahertz 2-frames per second standoff imaging

Thomas M. Goyette[*a], Jason C. Dickinson[a], Kurt J. Linden[b] , William R. Neal[b], Cecil S. Joseph[a], William J. Gorveatt[a], Jerry Waldman[a], Robert Giles[a], and William E. Nixon,[c]

[a]Submillimeter-Wave Technology Laboratory, University of Massachusetts Lowell, 175 Cabot St., Lowell, MA 01854;
[b]Spire Corporation, Bedford, MA 01730
[c]United States Army, National Ground Intelligence Center, 2055 Boulders Road, Charlottesville, VA 22911

ABSTRACT

A Terahertz imaging system intended to demonstrate identification of objects concealed under clothing was designed, assembled, and tested. The system design was based on a 2.5 m standoff distance, with a capability of visualizing a 0.5 m by 0.5 m scene at an image rate of 2 frames per second. The system optical design consisted of a 1.56 THz laser beam, which was raster swept by a dual torsion mirror scanner. The beam was focused onto the scan subject by a stationary 50 cm-diameter focusing mirror. A heterodyne detection technique was used to down convert the back-scattered signal. The system demonstrated a 1.5 cm spot resolution. Human subjects were scanned at a frame rate of 2 frames per second. Hidden metal objects were detected under a jacket worn by the human subject. A movie including data and video images was produced in 1.5 minutes scanning a human through 180° of azimuth angle at 0.7° increment.

Keywords: Terahertz, imaging, concealed, weapon

1. INTRODUCTION

Heretofore a number of terahertz imaging systems have been reported.[1,2] However, most of the reported systems require long exposure times to produce adequate images. The goal of this work is to show that it is practical to perform full body image scans at a near video frame rate. The source and receiver technology used in this scan were of a standard type that included optically pumped far-infrared lasers and room temperature Schottky diode receivers. The lasers and diodes were optimized to operate at 1.56 THz. An optical setup was designed to produce a focused spot for the transmitter and receiver to view the subject. Special electronics were designed to allow heterodyne detection. A raster scan was produced through the use of a commercially available scanning mirror. The resulting THz scan is shown in Figure 1. This scan took only 0.5 seconds and is a single frame out of a much larger data movie. The data acquisition rate was not limited by the sensitivity of the receiver but rather the mechanics of the scanner. The sensitivity of the setup was sufficient to allow video scan rates. A detailed description of the setup will be given in Section 2. The data from the complete movie is discussed in Section 3.

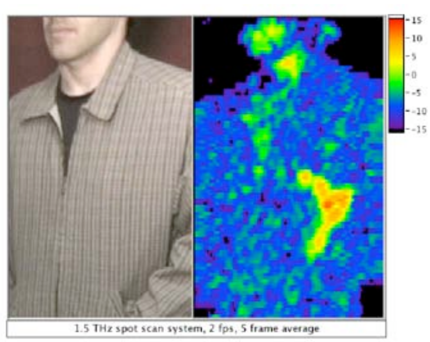

Figure 1. Sample THz image of concealed weapon scan in a dB color scale.

[*] Thomas_Goyette@uml.edu; phone 978 934-1380

Report Documentation Page

Form Approved
OMB No. 0704-0188

1. REPORT DATE **2008**	2. REPORT TYPE	3. DATES COVERED **00-00-2008 to 00-00-2008**

4. TITLE AND SUBTITLE **1.56 Terahertz 2-frames per second standoff imaging**	5a. CONTRACT NUMBER
	5b. GRANT NUMBER
	5c. PROGRAM ELEMENT NUMBER
6. AUTHOR(S)	5d. PROJECT NUMBER
	5e. TASK NUMBER
	5f. WORK UNIT NUMBER
7. PERFORMING ORGANIZATION NAME(S) AND ADDRESS(ES) **University of Massachusetts Lowell,Submillimeter-Wave Technology Laboratory,175 Cabot St,Lowell,MA,01854**	8. PERFORMING ORGANIZATION REPORT NUMBER
9. SPONSORING/MONITORING AGENCY NAME(S) AND ADDRESS(ES)	10. SPONSOR/MONITOR'S ACRONYM(S)
	11. SPONSOR/MONITOR'S REPORT NUMBER(S)

12. DISTRIBUTION/AVAILABILITY STATEMENT
Approved for public release; distribution unlimited

13. SUPPLEMENTARY NOTES

14. ABSTRACT
A Terahertz imaging system intended to demonstrate identification of objects concealed under clothing was designed, assembled, and tested. The system design was based on a 2.5 m standoff distance, with a capability of visualizing a 0.5 m by 0.5 m scene at an image rate of 2 frames per second. The system optical design consisted of a 1.56 THz laser beam, which was raster swept by a dual torsion mirror scanner. The beam was focused onto the scan subject by a stationary 50 cm-diameter focusing mirror. A heterodyne detection technique was used to down convert the backscattered signal. The system demonstrated a 1.5 cm spot resolution. Human subjects were scanned at a frame rate of 2 frames per second. Hidden metal objects were detected under a jacket worn by the human subject. A movie including data and video images was produced in 1.5 minutes scanning a human through 180° of azimuth angle at 0.7° increment.

15. SUBJECT TERMS

16. SECURITY CLASSIFICATION OF:			17. LIMITATION OF ABSTRACT	18. NUMBER OF PAGES	19a. NAME OF RESPONSIBLE PERSON
a. REPORT **unclassified**	b. ABSTRACT **unclassified**	c. THIS PAGE **unclassified**	**Same as Report (SAR)**	**11**	

Previous THz material and atmospheric studies,[3-7] including evaluation of multiple active THz radar systems at the National Ground Intelligence Center (NGIC) and the University of Massachusetts Lowell (UML), were used in determining the setup for the THz scanner. A frequency of 1.56 THz was chosen since it is located in one of the windows for transmission through the atmosphere where absorption of the power by water molecules is minimized[3], and its relatively high frequency should provide good resolution. Several such windows exist and are appropriate for use for THz scanning. UML has devices already optimized for 1.56 THz that are used for radar modeling. Since the data include scans of human subjects, permission was received from the UML Institutional Review Board (IRB) for human scanning. The data in this work was taken from November 2006 to February 2007 and is within the scope of UML IRB Number 06-1391 (expiration date June 2008).

2. EXPERIMENTAL SETUP

The Submillimeter-Wave Technology Laboratory at UML has developed coherent source/receiver systems that are capable of demonstrating video rate imaging at THz frequencies. These systems use either solid-state multipliers[4,5] (160 GHz and 520 GHz) or molecular lasers[6,7] (350 GHz and 1.56 THz). The current sizes of the molecular laser components make them unsuitable for a portable THz imaging system. But reconfiguring the system's optics is straightforward. The systems are very useful for demonstrating scan imaging and studying the issues related to the detection of concealed objects. Solid-state multiplier sources are much more compact and their operating frequencies are steadily increasing. Newer compact source technologies such as quantum cascade lasers (QCL) are approaching 1.0 THz operation from the high frequency side[8]. Therefore, the availability of compact, coherent THz sources can be expected to grow in the near future.

The lasers used as the frequency sources in this work have been described in detail previously.[6] The source consists of two 150 Watt, ultra-stable, grating-tunable CO_2 lasers, which are used as the optical pumps for the two far-infrared lasers. The CO_2 lasers are set to produce 9 μm (9P22 CO_2 laser line) and 10 μm (10R10 CO_2 laser line) wavelengths respectively. The outputs are then used to pump the laser transitions in the molecular gases difluoromethane (CH_2F_2) and methanol (CH_3OH) at 1.5626 THz and 1.5645 THz respectively. The far-infrared lasers produce Gaussian modes with 10 mm full width at half maximum (FWHM) and typically 100 mW of power. One laser is used as the transmitter while the other serves as the receiver local oscillator.

2.1 Optical Design

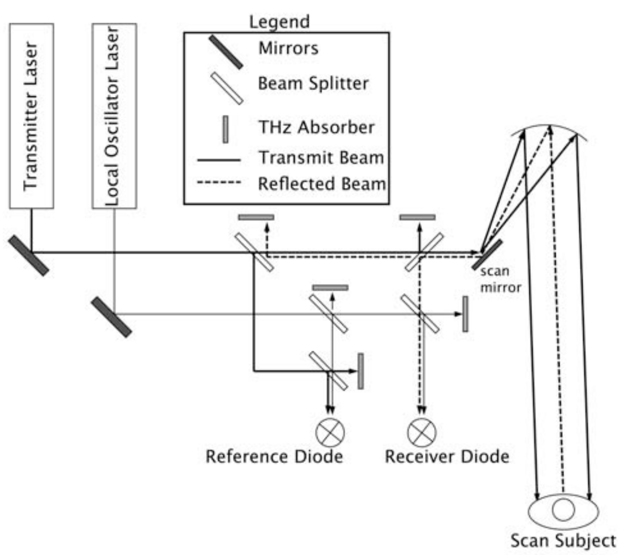

Figure 2. Block diagram of the optical design for the THz imaging system.

The optical design of the scanning system is shown in Figure 2. The local oscillator laser (LO) acts as the power source to produce the optimum bias on the reference and receiver diodes. The LO signal passes through a series of Mylar beam splitters in order to illuminate both diodes simultaneously. The transmitter laser also passes through a series of Mylar beam splitters. A small amount of the transmit power is combined with the LO signal on the reference diode. The remaining transmit power is directed through the beam splitters and steered with a scan mirror to allow a raster scan of the subject. Unused power from both lasers is deposited in THz absorbing material.

In addition to raster scanning the subject, the transmitter laser is focused to a small spot at the subject's location. This focusing is achieved by reflecting the transmitter laser off of a large-diameter focusing mirror. The focusing mirror consisted of a machined surface of 0.51 meter-diameter and 1.12 meter focal length. Since the frequencies involved are relatively low compared to optical frequencies, the effect of diffraction must be taken into account. The theory of Gaussian beams[9] has been used to calculate the exact positions for the optics in order to ensure that the field of view of the detector diode is overlapped with the transmitter beam. The system is designed to produce a two-way half power diameter of 7mm on the subject at a standoff distance of 2.54 meters.

2.2 Down-converting electronics

Figure 3 shows the block diagram of the down-converting electronics. The heterodyne down-conversion consists of a reference signal and a received signal. Both of these signals are generated by 1.5 THz corner-cube-mounted Schottky diodes. The reference diode and receiver diode in Figure 3 are the same as in Figure 2 but now are shown with the attached signal processing electronics. The reference diode creates a beat frequency of 1.86 GHz between the transmitter and receiver laser. This signal is used as a reference to measure both the amplitude and phase of the received signal. In order to convert the received signals into amplitude and phase information a lock-in amplifier is used.

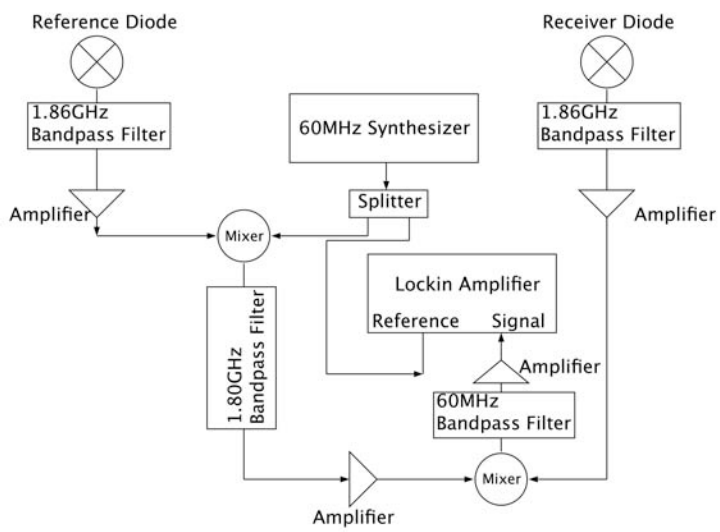

Figure 3. Block diagram of the down-converting electronics.

Since the difference frequency between the two lasers is 1.86 GHz, it is difficult to use a lock-in amplifier without further down-converting the frequencies. The reference signal is first shifted by 60 MHz to offset it from the signal from the receiver. The shifted reference signal is then mixed with the signal from the receiver in order to down-convert the signal to a stable 60 MHz frequency. The resulting signal is filtered and amplified before being sent into the lock-in. The 60 MHz synthesizer is also sent into the lock-in amplifier as the reference frequency. Thus, by this series of down-conversions the amplitude and phase information of the received signal is passed to a very stable synthesized frequency that is used as a carrier. This method has the effect of removing any slow frequency jitter from the lasers caused by mechanical/acoustic noise in the room.

2.3 Scanner mirror

A commercially available scanning mirror was used to produce the raster scan across the scan region. The scanning mirror is shown in Figure 4. The scanner consists of two optical-quality mirrors mounted on galvanometric motors that are set orthogonal to one another. The transmit beam passes through the scanner by reflecting off of the lower mirror and then the upper mirror. The lower mirror is used as the fast scan axis and rapidly scans the horizontal direction. The upper mirror is the slow scan axis and scans the vertical direction. The vertical direction is scanned at a rate of 2 Hz while the horizontal direction has a scan rate of 200 Hz. The scanner can produce images at a frame rate of 2 frames/second. Currently the frame rate is dependent on the physical limitations of the fast scanning mirror. A special circuit was designed to control the scan motors and to provide trigger pulses for data collection.

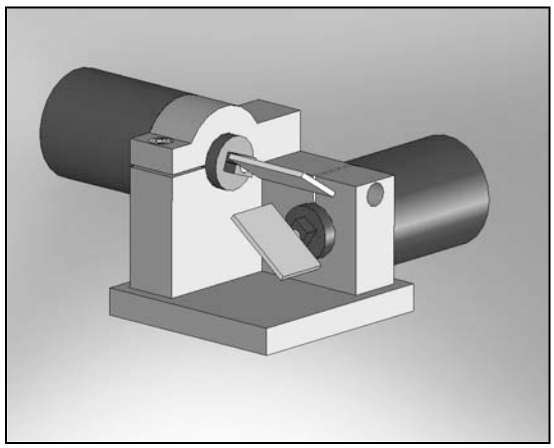

Figure 4. Commercial scanning mirror.

2.4 Image construction

Data acquisition and processing software was written using National Instrument's LabVIEW software. In order to provide a side-by-side comparison between the visible image and the THz imagery, a video camera was placed slightly off axis from the THz measurement path. A video frame was captured simultaneously with each frame of the THz scan. THz images typically consist of a 200 point by 100 point grid requiring 20,000 complex data points per scan. This results in a data collection rate of 40 kHz for frame rates of 2 frames per second. Complex amplitude and phase information were converted to voltages by a lock-in amplifier* with the time constant turned off, resulting in an effective data bandwidth of approximately 100 kHz. A circuit was designed and built to drive the galvanometers for the scanner shown in Figure 4. The 200 pixel by 100 pixel resolution remained fixed. However, the effective scan area was variable by tuning the driver circuit.

Effective scan areas of 0.51 meter by 0.51 meter could be achieved. However, since the fast scan axis was required to oscillate back and forth at a rapid rate it was found that excess heat was produced in the motors, which ultimately caused problems with position accuracy. Additionally, since the galvanometer must speed up and slow down at the ends of each horizontal scan, distortions of the images around the edges were observed. Ideally, a position driven data collection method would overcome this effect. However, since a position encoder was not available for the scanner it was necessary to rely on a single trigger pulse to initiate the 20,000 point data collection. The velocity of the scanning mirror

* Stanford Research Systems Model 844

is illustrated in Figure 5. Since the scan is bi-directional, an asymmetry occurs between left sweep and right sweep velocities.

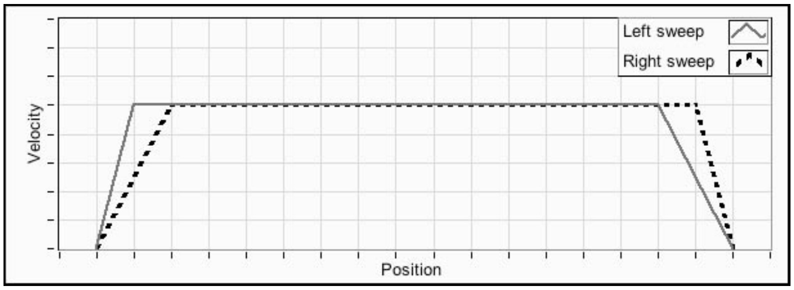

Figure 5. Theoretical velocity profile of the fast scan axis. The two traces indicate theoretical left and right sweeps of the galvanometric actuator and fast scan mirror.

It was found that the distortions were reproducible enough to allow straightforward image correction algorithms to be applied. Figure 6 shows the result of this algorithm. A sample scan was performed on a hand and an image was generated using a constant shift between left scan and right scan rows. The center image shown in Figure 6 is made by using this simple technique. The right image shows the result of applying an algorithm to correct for the asymmetry in velocity at the ends of the horizontal sweeps. Note that the overshoot problem is now corrected for and produces a clearer image.

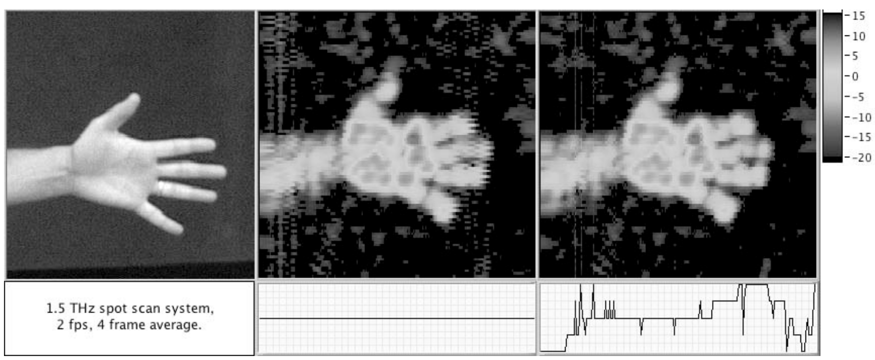

Figure 6. Still frame of the target subject (left), the simple even-lines-rotated image (center), and the scanner overshoot corrected image (right). Note the clarity of the rightmost frame. The graph below each image shows the correction applied.

3. RESULTS

3.1 Test of primary mirror

Figure 7 shows the results of tests performed on the primary focusing mirror. The focusing mirror consists of an Aluminum plate machined on a CNC lathe so that the front surface has the required radius of curvature for a 1.12 m focal length. A test pattern is shown in Figure 7 as a series of straight helium-neon laser lines that is produced by steering a helium-neon laser through the scanner mirror and scanning a square area the size of the focusing mirror. The test scan is reflected off of the focusing mirror and projected onto a white screen in order to determine the effects of machining marks on the mirror. The result in Figure 7 is the right most image, showing the convolution of the original test scan and the surface quality of the machined surface. Although it appears at first glance that the quality of the machined surface may be a problem, it is useful to remember that since the test is performed with an optical beam the distortions produced by the machine marks are exaggerated compared to the effect that will be observed at 1.56THz with a corresponding wavelength of 191 μm. At 1.56 THz the roughness of the surface is within tolerance for use as a focusing mirror. However, it will be shown in the next section that the distortions on the surface of the focusing mirror ultimately limit the focusing of the scan spot at the target location.

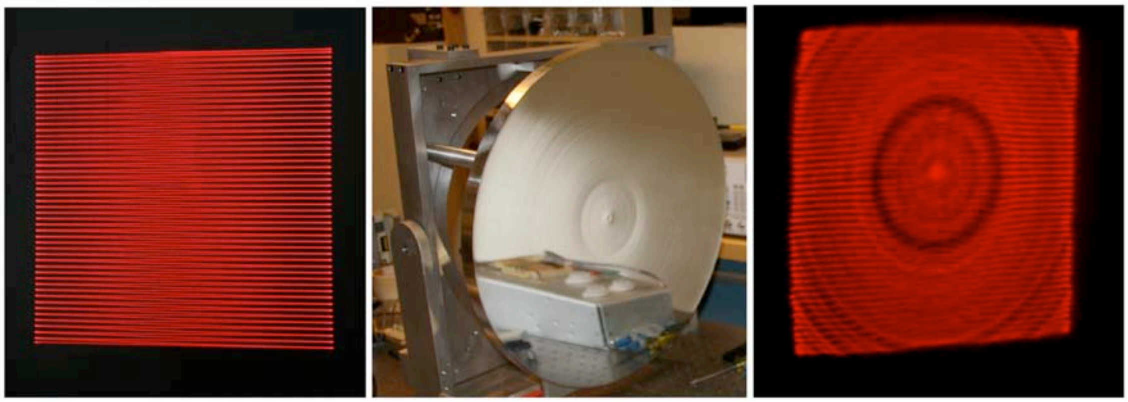

Figure 7. Test results of primary focusing mirror are shown. The left image is a Helium-Neon test scan pattern. The center image is the machined focusing mirror. The right image is the test pattern after reflecting off of the focusing mirror and projected on a white screen.

3.2 Beam Diagnostics

In order to determine the best optical design for the THz imager, Gaussian beam calculations were used to simulate different optical configurations. Extensive beam scans were performed at each step to ensure that the focusing and expansion of the LO and Transmitter laser beams followed the predicted parameters. The scans included both one-dimensional and two-dimensional scans with Gaussian beam waists fit with a least square analysis. After each optic was put into place the expansion of the laser beams were measured and compared to the predicted beam waists. A final measure of the beam quality and field of view of the system was to scan a 1.5mm diameter dihedron across the focused spot at the position where the subject is to be scanned. The back reflected signal was then collected by the receiver diode and down-converted to amplitude and phase information for post analysis. Figure 8 shows the results for the 2-dimensional mode scans when scanning the dihedron at the target location.

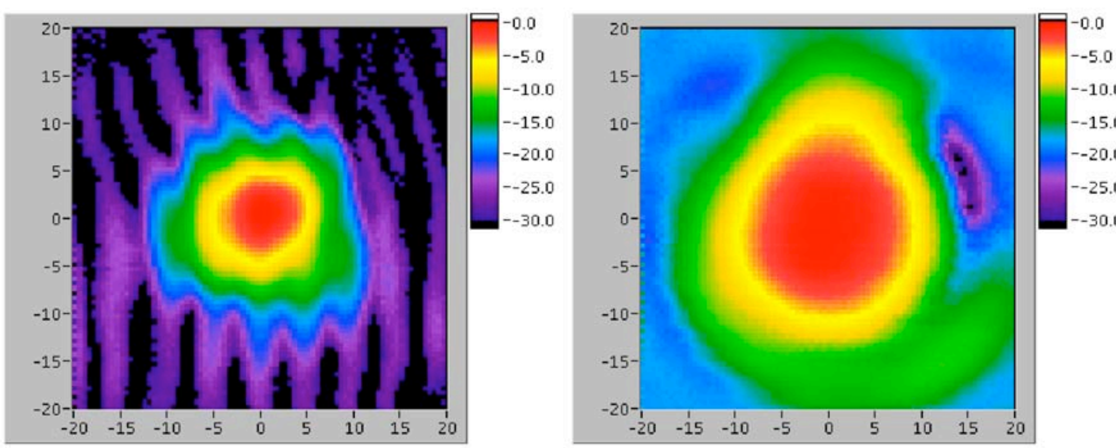

Figure 8. A comparison of 2 way beam scans shows the size of the focused spot when an optical-quality focusing mirror is used (left) and when the large machined surface focusing mirror is used (right). The machined surface ultimately proved to be a limiting factor for focused spot size. Color scale is in dB. Distance is displayed in mm.

The left side figure shows the focused spot scan after reflecting the laser off of an optical quality mirror of the same focal length as the machined mirror. The right side figure is the same type of scan but now the optical quality mirror is replaced with the machined focusing mirror. Originally, the optical quality mirror was used only to align the system while the larger machined mirror was being made. However, it did prove useful to test the focusing of the system prior to replacing it with the machined mirror. It can be seen that simply changing the mirror caused the focus to widen by about a factor of two. This result is not surprising since the machined mirror was of an inexpensive type. A better quality surface is recommended for such mirrors in future work. The Full Width at Half Maximum (FWHM) size of the focused spot was measured to be 7 mm when reflected from the optical mirror. The FWHM focused spot was measured to be 14 mm when the machined mirror was used. The diffractive ripple observed in Figure 8 in the horizontal direction is a result of a slightly under-sized horizontal scanning mirror that allowed some of the transmit beam to scatter off of the edges. The data in Figure 8 were taken by reflecting the transmitter beam off the center of both mirrors. Similar results were observed when other parts of the machined mirror were probed.

3.3 Final THz scanner parameters

Table 1. Final THz scanner operating parameters.

Polarization	Horizontal at Target
Data	Complex(I and Q)
Spot Size	1.5 cm(FWHM)
Signal to Noise	100dB (30KHz RBW)
Scan Speed	2 frames/second
Standoff Distance	2.54 meters
Scan Diameter	0.51 meters(max)

The final parameters for the THz scanner are listed in Table 1. Polarization sensitivity was measured by using a wire grid polarizer. Since the corner-cube-mounted Schottky diodes rely on vertical antennas the wire grid test confirmed that the receiver is sensitive to vertical polarization. However the steering mirror re-polarizes the radiation to horizontal. The heterodyne down-conversion allows both the amplitude and phase of the data to be measured, giving a complex data stream. The spot size as determined in the previous sections was averaged for measurements across the entire surface of the focusing mirror resulting in 1.5 cm FWHM. Signal to noise measurements were made by reflecting the entire power of the transmitter back from the target region by using a trihedron. This method allowed the measure of the down-converted power of the full power of the laser when passing through all of the optical setup and was measured to be +5 dBm on a spectrum analyzer. In terms of radar cross-section, a 1.5 cm spot size corresponds to a 10 dBm^2 object at 1.56 THz. The noise floor of the electronics was also measured on the spectrum analyzer as -95 dBm in a 30 KHz resolution bandwidth (RBW). The result is a signal-to-noise ratio of 100 dB in 30 KHz RBW. The noise floor for this measurement was limited by the noise of the spectrum analyzer. Frame scan rates of 2 frames/second were observed with a standoff distance of 2.54 meters. The scan area was limited to the size of the mirror at 0.51 meters diameter.

3.4 Scanning of human subject

After diagnostic tests were performed on the THz scanner, scans of human subjects were performed. Due to the limitations of the fast scanning mirror described in Section 2.4 it was necessary to limit the size of the scan in the horizontal direction. In order to maintain a scan rate of 2 frames/second the horizontal scan width at the target area was reduced to 0.33 meters. This limitation can be relaxed at slower scan rates and it is likely that a scanning mirror optimized for this purpose will also provide larger scan regions.

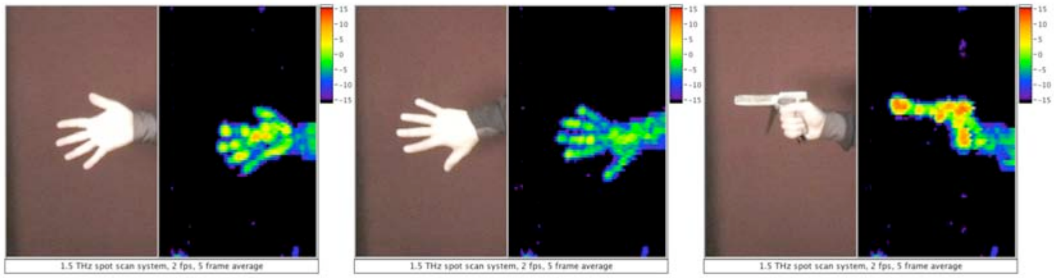

Figure 9. Sample images of a hand and cable tie gun at a scan rate of 2 frames/second. Color scale is in dB.

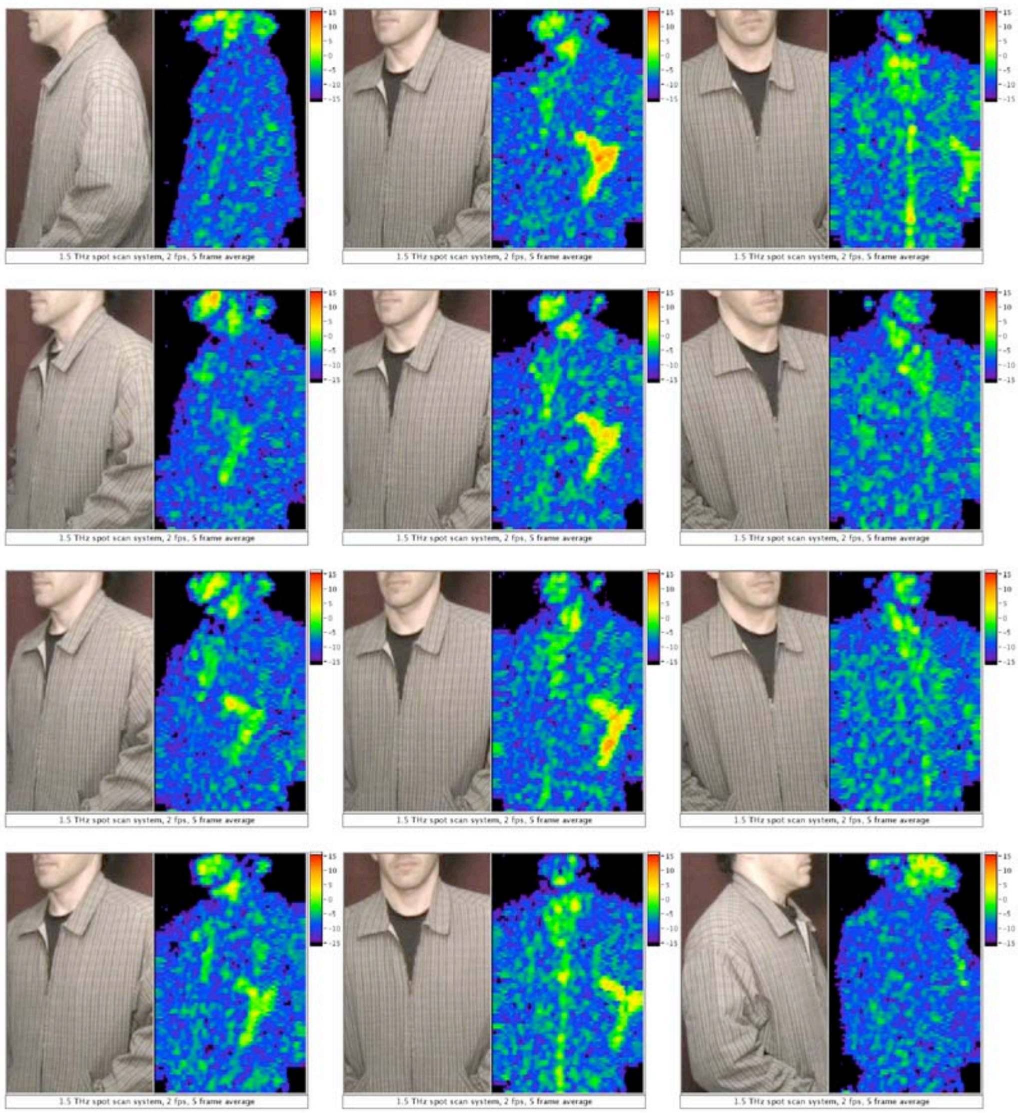

Figure 10. Sample images of a person with cable tie gun hidden under jacket. Color scale is in dB.

Figure 9 shows a sample scan of a human hand. The image was produced by scanning the target region using a scan distance of 0.33 meters horizontal and 0.53 meters vertical. The frames shown in Figure 9 are from a much larger data movie. Once the THz scanner is set to scan, the data collected is streamed to the computer disk. In addition to the data that is recorded from the down-converting electronics, a video camera is mounted slightly above the large focusing mirror and monitored simultaneously. When each frame of THz data is collected the image from the video camera is stored along with it. The result is a movie that shows both the video image of the target and the THz scan correctly synchronized.

The data shown in Figure 9 are displayed in false color on a dB scale in power. The image is shown with 30dB of dynamic range, however the noise floor is substantially lower than what is displayed. Due to scattering from the scanner body there is an unwanted constant background signal that limits the lower levels on the display. Signal analysis has been used to reduce this effect, but since the signal varies with the scanner position it was not eliminated entirely. This dynamic range is more than enough to allow good quality images to be produced. Figure 10 shows a series of images similar to that of Figure 9 from a data movie taken on a human volunteer. The scan region was enough to allow the torso to be viewed. The volunteer wore a light jacket with the cable tie gun hidden in the inside pocket. To form this image the volunteer stood on a rotating stage while the scanner collected the movie. The movie extends to 180˚ of azimuth turn and took approximately 1.5 minutes to generate.

4. DISCUSSION

Many data movies similar to those displayed in Figure 9 and Figure 10 were recorded. The images in Figure 9 show that for the hand without the gun there are regions of high reflectivity. This is not surprising since the reflectivity of skin is about 15% in the THz frequency region. In the image of the hand holding the gun the features of the gun are much more efficient at back-scattering power than the hand alone. Likewise the material of the shirt (polypropylene) did not show very strong backscatter. However, that is likely due to the irregular surface features.

Figure 10 shows some interesting scattering features with respect to the gun. The movie in Figure 10 is taken with the volunteer facing to the left of the image and scanned over a half spin of 180˚. The gun is placed in the inside breast pocket of the jacket. It is clear that a useful amount of power, estimated at 0.5m W/cm^2 on the target, was able to penetrate the light cotton jacket (0.7 mm thickness) and scatter from the gun. The gun appears to persist over a large number of azimuth angles with the very strong return when it is at a nearly normal angle of incidence. However, the plastic encased trigger is not observed. The jacket itself does not return more than a diffuse signal except where the zipper is located. Both the zipper and the clasp do give a stronger return at some angles.

Previous studies have shown that penetration of THz radiation through common clothing materials is dependent on both frequency and material.[10] Penetration of clothing has been observed to be higher at 325 GHz[1] however, resolution diminishes in general at lower frequencies and therefore the optimum balance must be found. Figure 11 shows a sample scan of transmission and reflection through cotton fabric in the THz frequency region. Note that the transmission through cotton has a significant variation from low frequency to high frequency. However, the reflection from cotton is relatively constant across the THz frequency region, averaging less than 1%. The small reflectivity explains why the material shows only diffuse scattering. During the test scans the power return observed on the spectrum analyzer was measured to be -60 dBm for the diffuse scattering of the jacket. For a material that scatters diffusely in all directions, a radar cross-section of -57 dBm^2 is expected for a 1.5 cm spot of 1% reflectivity such as the jacket. Using the results of Section 3.3 for reflection from the trihedron, a power measure of -62 dBm is expected from the spectrum analyzer. This is good agreement with the measured number of -60 dBm. The results will in general vary with material. Many other materials have been studied previously and have shown similar variations.[10]

It was shown in Figure 8 that the machining quality of the focusing mirror was the limiting factor for focused spot size. However, even with this constraint the optical system produced a focused spot that was adequate for purposes of video imaging. A mirror that did not have this effect could produce a factor of 2 better image resolution at the same scan rate. One benefit of the larger spot size is that the field of focus is effectively doubled. This effect provides a much more robust system that is not as dependent on the exact standoff distance to the target.

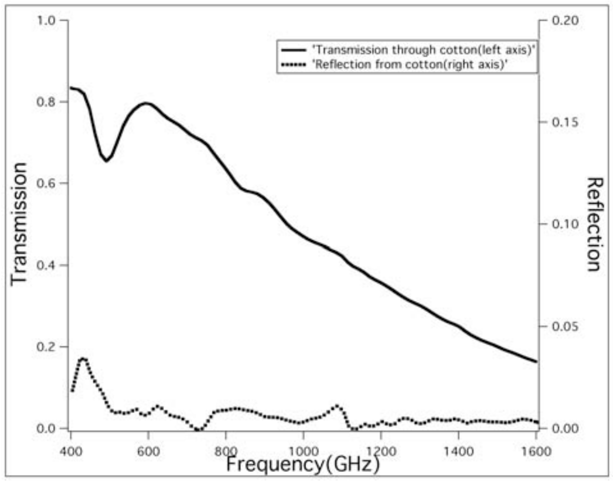

Figure 11. Transmission and reflection of THz radiation through cotton fabric.

The images of Figure 10 are displayed with a simple logarithmic power plot. In these images the phase of the signal was not used except to eliminate the constant background, although the phase was recorded. Since the data can be over-sampled it becomes possible for a more complex analysis similar to the analysis of Synthetic Aperture Radar (SAR) data. It can be shown that moving a focused spot across the target and over-sampling the system is identical to the scanning of a radar beam across a target scene. The mathematics of SAR then becomes applicable. Using the amplitude and phase information in such an analysis could provide enhanced resolution with no reduction in speed.

5. SUMMARY

A Terahertz imaging system for identification of objects concealed under clothing was demonstrated. The system design was based on a 2.5 m standoff distance, with a capability of visualizing a 0.5 m by 0.5 m scene at an image rate of 2 frames/second. The Terahertz scanner final parameters are nearly equal to predictions using Gaussian beam theory. The scan parameters are limited only by the physical speed of the torsion scanner and the surface quality of the focusing mirror. A heterodyne detection technique was used to down convert the back-scattered signal into both amplitude and phase information. Data collection and analysis software was written and optimized for real time image display. The system demonstrated a 1.5 cm FWHM spot resolution. Human subjects were scanned at a frame rate of 2 frames/second. Hidden metal objects were detected under a jacket worn by the human subject. Data movies are produced with optical images collected simultaneously and displayed for image comparison

ACKNOWLEDGEMENTS

This work was funded as a Phase II effort through the Department of Homeland Security (DHS) Science and Technology (S&T) Small Business Innovation Research (SBIR) Program. The authors gratefully acknowledge the technical support of Peter Costianes of the U. S. Air Force Research Laboratory (AFRL) Information Directorate, the project technical monitor, and Trent DePersia of the Department of Homeland Security. This work was also supported by U. S. Army National Ground Intelligence Center contract numbers DASC0101C0011 and W911W406C0020.

REFERENCES

1. J. C. Dickinson, T. M. Goyette, J. Waldman,"High Resolution Imaging using 325GHz and 1.5THz Transceivers", *Fifteenth International Symposium on Space Terahertz Technology* (STT2004), April 27-29, 2004, Northampton, MA
2. J. C. Dickinson, T. M. Goyette, A. J. Gatesman, C. S. Joseph, Z. G. Root, R. H. Giles, J. Waldman, and W. E. Nixon,"Terahertz imaging of subjects with concealed weapons", in *Terahertz for Military and Security Applications IV*, edited by Dwight L. Woolard, R. Jennifer Hwu, Mark J. Rosker, James O. Jensen, Proceedings of the SPIE Vol. 6212
3. K. J. Linden, W. R. Neal, J. Waldman, A. J. Gatesman, and A, Danylov, "THz laser based standoff imaging system", IEEE Computer Society, *Proceedings of the 34th Applied Imagery Recognition Workshop*, April 2005, Washington, D. C., p7-14.
4. M. J. Coulombe, T. Horgan and J. Waldman, J. Neilson, S. Carter and W. Nixon,"A 160 GHz Polarimetric Compact Range for Scale Model RCS Measurements", Antenna Measurements and Techniques Association (AMTA) Proceedings, Seattle, WA, pg 239, October 1996.
5. M. J. Coulombe, T. Horgan and J. Waldman, G.Szatkowski , and W. Nixon,"A 520 GHZ Polarimetric Compact Range for Scale Model RCS Measurements", Antenna Measurements and Techniques Association (AMTA) Proceedings, Monterey, October 1999.
6. T. M. Goyette, J. C. Dickinson, J. Waldman, and W. E. Nixon, "A 1.56THz compact radar range for W-Band imagery of scale-model tactical targets", *Proceedings of SPIE, Algorithms for Synthetic Aperture Radar Imagery VII*, Vol. **4053**, p615-622, 2000.
7. T. M. Goyette, J. C. Dickinson, W. J. Gorveatt, J. Waldman, W. E. Nixon ,"X-band ISAR imagery of scale-model tactical targets using a wide-bandwidth 350-GHz compact range", Proc. SPIE Vol. **5427**, p. 227-236, *Algorithms for Synthetic Aperture Radar Imagery XI*; Edmund G. Zelnio, Frederick D. Garber; Eds. September 2004.
8. C. Walther, M. Fischer, G. Scalari, R. Terazzi, N. Hoyler, and J. Faist, "Quantum cascade lasers operating from 1.2 to 1.6 THz", *Applied Physics Letters* **91**, 2007.
9. A. Yariv, *Quantum Electronics, Second Edition*, John Wiley and Sons, Inc, New York, New York USA, 1975, p109-127.
10. A. J. Gatesman, A. Danylov, T. M. Goyette, J. C. Dickinson, R. H. Giles, W. Goodhue, J. Waldman, W. E. Nixon, and W. Hoen,"Terahertz Behavior of Optical Components and Common Materials", in *Terahertz for Military and Security Applications IV*, edited by Dwight L. Woolard, R. Jennifer Hwu, Mark J. Rosker, James O. Jensen, Proceedings of the SPIE Vol 6212. May 2006